Chemistry–A European Journal

Research Article
doi.org/10.1002/chem.202501877

Chemistry
Europe
European Chemical
Societies Publishing

www.chemeurj.org

A Tour in the Chemistry of a Tricoordinate Rh(−I) Complex

Víctor Varela-Izquierdo,[a] José A. López,[a] Miguel A. Ciriano,*[a] and Cristina Tejel*[a]

The finding of the unprecedented 16-e tricoordinate planar rhodium(−I) complex, K[Rh(IPr)(dvtms)] (K[**1**]) (IPr = 1,3-bis(2,6-diisopropylphenyl)imidazolyl-2-ylidene, dvtms = divinyltetramethyldisiloxane) prompted us to explore its reactivity. K[**1**] reacts as a nucleophile with methyliodide to give [Rh(IPr)(dvtms)Me], a Rh(I) compound with an exceptional trigonal-pyramidal structure. Other haloalkanes abstract one electron from K[**1**] to give the previously reported [Rh⁰(IPr)(dvtms)] complex. K[**1**] also reacts with protonic acids and weak proton sources such as water and ketones to eventually give the rare tricoordinate 14-electron complex [Rh^I(IPr)(SiMe$_2$OSiMe$_2$CH = CH$_2$)] with a Rh −Si bond. The 16-electron complex [Rh^I(IPr)(SiMe$_2$OSiMe$_2$CH = CH$_2$)(H$_2$C = CH$_2$)] was characterized as an intermediate in this reaction. Furthermore, K[**1**] runs up to five cycles of catalytic condensation of nonenolizable aldehydes to esters, such as p-tolylaldehyde, before being fully converted into the inactive complex Rh(IPr)(η^3-C$_3$H$_4$^{p}tolyl)(C$_2$H$_4$)] with fragmentation of the diolefin dvtms. Computational studies have provided valuable insights into the reactivity patterns and behavior of this complex, including those of the rhodium(−I)/rhodium(I) catalytic cycle.

1. Introduction

Low-valent, low-coordinated complexes are intriguing compounds due to their unique electronic structures and reactivity and may attract significant interest for their potential in catalysis.[1–7] These properties offer new possibilities for catalytic processes that are difficult or unattainable with traditional catalysts.[8–10] Additionally, they provide valuable insights into fundamental chemistry.

In this context, the chemistry of rhodium complexes in low oxidation states (0 and − I) has received surprisingly limited attention in spite of being known for over 50 years. Examples include chemically or electrochemically generated d⁹-[RhL₄]• species stabilized by π-acidic ligands.[11–19] However, well-defined, isolated paramagnetic rhodium(0) complexes remain rare, with only a few examples reported.[20–26] DFT calculations on these species revealed relatively low spin density at the rhodium center, typically between 20% and 50%, indicating that most of them are better described as delocalized radicals.[16,25]

Notable exceptions are [Rh(trop₂dad)]• (trop₂dad = 1,4-bis(5H-dibenzo[a,d]cyclohepten-5-yl)-1,4-diazabuta-1,3-diene), which is clearly the ligand-centered radical [Rh^I(trop₂dad•⁻)],[24] whereas [Rh(IPr)(dvtms)]• (IPr = 1,3-bis(2,6-diisopropylphenyl)imidazolyl-2-ylidene, dvtms = divinyltetramethyldisiloxane) is the unique true metalloradical Rh(0) complex.[26] Additionally, [Rh(trop₂PPh)(PPh₃)]• (trop = 5H-dibenzo[a,d]-cyclohepten-5-yl) exists as a metalloradical in rapid equilibrium with its "ligand radical" electromer.[17]

Mononuclear Rh(−I) complexes, [RhL₄]⁻, are even rarer. Most of them are tetracoordinated species that follow the 18-electron rule.[27–38] Crystallographic studies reveal that these complexes typically adopt tetrahedral or near-tetrahedral structures. Two notable exceptions are our recently reported 16-electron, tricoordinate planar complexes [Rh(L)(dvtms)]⁻ (L = IPr, PPh₃),[26] and [Rh(CNAr^{dipp})₃]⁻ (Ar^{dipp} = 2,6-(^{i}Pr₂C₆H₃)₂C₆H₃).[39] A key distinction between them is the strictly trigonal-planar geometry of the former, whereas the latter adopts a pronounced Y-shaped structure in solid state and in solution.

The reactivity of low-valent rhodium complexes, especially the paramagnetic ones, is not well understood and can be obscured by disproportionation reactions: 2 [Rh⁰] → [Rh^I] + [Rh$^{−I}$], which generate more reactive species. For example, this reaction occurs rapidly for [Rh(tropp^{Ph})₂] (tropp^{Ph} = 5-diphenylphosphanyldibenzo[a,d]cycloheptene).[40] Despite this, a common behavior of d⁹-rhodium species is their ability to abstract hydrogen from proton sources[12,13b,13c,14] making them promising candidates for both mono-[41] and dinuclear[42] C − H activation reactions, as well as catalysts for photolytic water splitting.[43] In some cases, chloride abstraction has been observed,[15b] and molecular hydrogen cleavage into rhodium hydrides has been achieved, as demonstrated by [Rh(dppe)₂]• (dppe = 1,2-bis(diphenylphosphino)ethane) and [Rh(CO)(PPh₃)₃]•.[12,13a] Additionally, this complex readily undergoes ligand substitution of PPh₃ by NO and CO.[12]

Although little is known about the chemistry of diamagnetic d¹⁰-rhodium(−I) complexes, some studies have revealed their nucleophilic metal character. For example, protonolysis of [Rh(dppe)₂]MgCl leads to the corresponding hydride complex,

[a] Dr. V. Varela-Izquierdo, Dr. J. A. López, Prof. M. A. Ciriano, Prof. C. Tejel
Departamento de Química Inorgánica, Instituto de Síntesis Química y Catálisis Homogénea (ISQCH) CSIC-Universidad de Zaragoza, Pedro Cerbuna 12, Facultad de Ciencias, Zaragoza 50009, Spain
E-mail: mciriano@unizar.es
ctejel@unizar.es

Chemistry–A European Journal

Research Article
doi.org/10.1002/chem.202501877

Chemistry Europe
European Chemical
Societies Publishing

and it reacts with methyl iodide to form [Rh(dppe)₂(Me)]. However, exposure of [Rh(dppe)₂]MgCl to main-group electrophiles, such as Me₃SnCl, results in an unexpected transformation of the intermediate [Rh(dppe)₂(SnMe₃)] into [Rh(dppe)₂(H)].[33a] In contrast, adducts are successfully formed in reactions of [Rh(tmbp)₂]⁻ (tmbp = 4,4′,5,5′-tetramethyl-2,2′-biphosphinine) and [Rh(CO)₂(PPh₃)₂]⁻ with Ph₃SnCl[34] and Me₂SnCl₂,[30] respectively.

Oxidative addition has been observed in two cases: C − CN bond cleavage of benzonitrile[44] and C − N bond cleavage in IMes (IMes = 1,3-bis(2,4,6-trimethylphenyl)imidazolyl-2-ylidene).[45] Additionally, the highly reactive [Rh(dppe)₂]MgCl.[33a] has shown activity in CO₂ reduction. Pioneering work by Ragaini et al. demonstrated the effectiveness of [Rh(CO)₄]⁻ as a catalyst for nitroaromatic reduction and carbonylation.[46] More recently, a formal Rh⁻ᴵ/Rhᴵ redox cycle was identified in the catalytic hydrogenolysis of aryl C − F bonds.[47]

Despite significant progress, much remains unexplored in the chemistry of d¹⁰-rhodium(−I) complexes, particularly those with low coordination numbers. Coordinative unsaturation is expected to greatly enhance their reactivity compared to their saturated, tetracoordinate counterparts. The preceding studies on [Rh(CNAr^dipp)₃]⁻ revealed its ability to undergo protonolysis, to bind thallium, and to give reactions with electrophiles such as trimethylsilyl triflate and hexamethyldisilane.[39]

In this work, we report the reactivity of our recently described tricoordinate rhodium(−I) complex, K[Rh(IPr)(dvtms)] (K[**1**]), with electrophiles such as methyl iodide, proton sources, ketones, and aldehydes.

2. Results and Discussion

A distinctive feature of the K[Rh(IPr)(dvtms)] (K[**1**]) complex is the strictly trigonal coordination of the rhodium atom, with a sum of bond angles around rhodium (Σ^0Rh) of 359.97(6), based on the midpoints of the C = C double bonds. Unlike the typical perpendicular coordination of the C = C bonds to the molecular plane in rhodium(I) complexes, the two C = C bonds in the chelating dvtms ligand ($H_2C = CHSiMe_2 − O − SiMe_2C = CH_2$) lie within the coordination plane.[26]

To further investigate its electronic structure, we performed a detailed DFT analysis. The results show that the HOMO is almost entirely derived from the rhodium dz^2 orbital (∼100%) and oriented perpendicular to the molecular plane (defined as the xy plane, Figure 1).

The HOMO-1 and HOMO-2 are primarily the metal dxz and dyz orbitals (e″ set in D_{3h} symmetry). In contrast, HOMO − 3 and HOMO − 4 are mixed dx^2-y^2 and dxy orbitals (e′ set in D_{3h} symmetry) coupled with the $\pi*$ orbitals of the C = C bonds. This interaction stabilizes the dx^2-y^2 and dxy orbitals relative to the dxz and dyz orbitals, revealing the covalent character of the Rh − dvtms bonds.[3] The difference with the other metal orbitals arises mainly from strong metal-olefin π-back donation, which is maximized in the xy plane. This contrasts with the related complex K[Rh(CNAr^dipp)₃], which has the HOMO derived
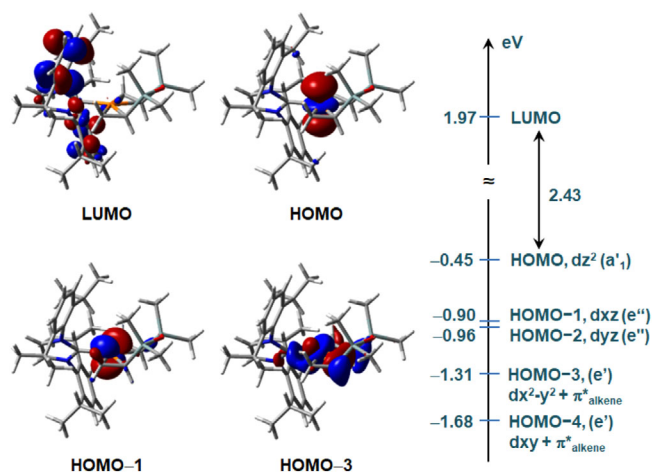

Figure 1. LUMO, HOMO-3, HOMO-1, and HOMO of K[**1**].
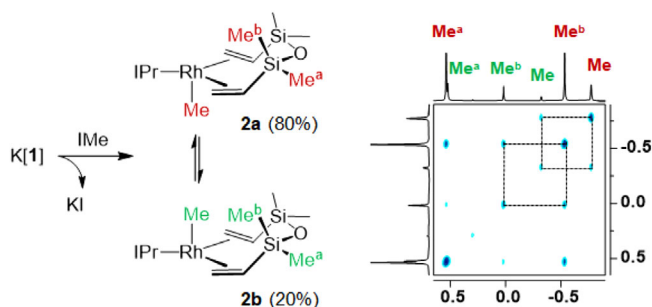
Figure 2. Synthesis of [Rh(IPr)(dvtms)(Me)] (**2**) from [Rh(IPr)(dvtms)] (K[**1**]). A selected region of the ¹H,¹H-exsy NMR spectrum is shown on the right.

from the dx^2-y^2 orbital.[39] As a result, K[Rh(IPr)(dvtms)] (K[**1**]) is expected to exhibit strong nucleophilic behavior.

NBO analysis shows a negative charge on both the rhodium atom (−0.36) and the olefinic carbons, particularly on the HC = carbons (−0.83 and − 0.84), compared to the H₂C = carbons (−0.51). This calculation indicates that the rhodium center and the olefinic bonds are likely reactive sites for electrophiles.

As expected, K[**1**] reacts immediately with the typical electrophile, MeI, to yield the oxidative semi-addition (oxidative ligation) product [Rh(IPr)(dvtms)(Me)] (**2**) and potassium iodide. Quantitative conversion was observed by ¹H-NMR spectroscopy (Figure 2). On a preparative scale, complex **2** was isolated from toluene as an orange solid with a good yield (60%), and single crystals were grown from a hexane solution cooled to − 35 °C.

The X-ray structure of complex **2** (Figure 3) reveals a tetracoordinated rhodium center in a trigonal pyramidal (TP) geometry, with the methyl group at the apex. There are two independent molecules in the asymmetric unit, with similar configurations.

This structure closely resembles that of [(Ph₃P)Au − Rh(dvtms)(IPr)] if the methyl group is formally replaced by its isolobal fragment [Au(Ph₃P)].[26] Consequently, the bond distances and angles are similar.

Notably, the TP geometry for a rhodium(I) complex is extremely rare, with very few examples reported: [Rh(trop₂SiMe)(L)] (L = C₂H₄, PPh₃, both by Grützmacher,[48] as well as [Rh(L){η³-Ge₉(Hyp)₃}] (Hyp = Si(SiMe₃)₃),[49] and

Chem. Eur. J. **2025**, *0*, e202501877 (2 of 9)

© 2025 The Author(s). Chemistry – A European Journal published by Wiley-VCH GmbH

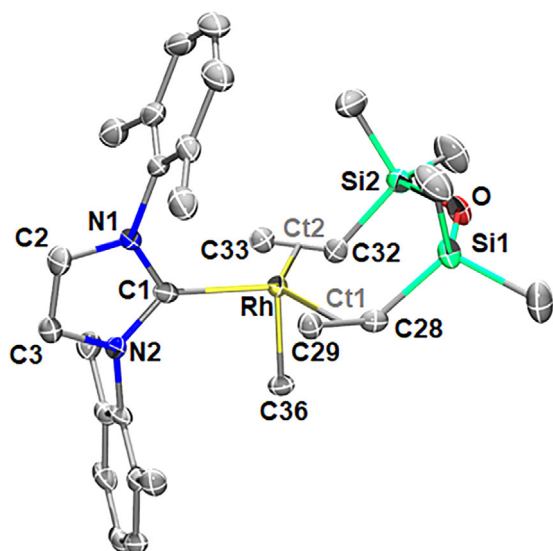**Figure 3.** Molecular structure (ORTEP, ellipsoids set at 50% probability) of complex [Rh(IPr)(dvtms)(Me)] (**2**). Selected bond distances [Å] and angles [°]: Rh — C1 2.139(5)/2.114(5), Rh — Ct1 2.030(5)/2.035(5), Rh — Ct2 2.039(6)/2.037(6), Rh — C36 2.028(5)/2.037(5), C28 — C29 1.416(7)/1.428(7), C32 — C33 1.436(7)/1.424(8), C1 — Rh — Ct1 108.3(2)/112.3(2), C1 — Rh — Ct2 118.6(2)/114.9(2), Ct1 — Rh — Ct2 133.0(2)/132.7(2), C1 — Rh — C36 96.2(2)/95.8(2). Only CH carbons of the iPr groups are shown for clarity.

[Rh(CNAr^{dipp})$_3$Tl].[39] In all these cases, the group with higher *trans* influence occupies the apical position.

NMR analysis of complex **2** shows an equilibrium in solution between two isomers (major isomer **2a** and minor isomer **2b**, Figure 2). Both isomers exhibit a plane of symmetry, which renders the two halves of the dvtms ligand equivalent. The methyl groups bound to rhodium appear as doublets in the ^{1}H and ^{13}C{^{1}H} NMR spectra (J(H,Rh) = 2.1 Hz, **2a**; 2.2 Hz, **2b**; J(C,Rh) = 31 Hz, **2a**; 32 Hz, **2b**). Additionally, bonding to rhodium causes a high-field shift for the corresponding carbons ($\delta = -1.6$ for **2a**, -1.0 ppm for **2b**). These observations align with the structures shown in Figure 2, in which the isomers differ in the position of the methyl group relative to the folding of the metallacycle.

The equilibrium between **2a** and **2b** is slow enough to be detected by the ^{1}H,^{1}H-exsy NMR spectrum (Figure 2). While the stereochemistry of **2a** and **2b** cannot be definitively determined from these spectra, it is likely that the major isomer (**2a**) corresponds to the solid-state structure. DFT calculations indicate that **2a** is 0.7 kcal mol^{-1} more stable than **2b**, whereas the square-planar configuration (**2c**) is positioned 1.2 kcal mol^{-1} above **2a**.

This isomerization, mediated probably through a square-planar species, involves a change in the orientation of the diolefins: they lie in the trigonal plane in **2a** and **2b**, but they are perpendicular to the molecular plane in the square-planar configuration.

Other electrophiles, such as dichloromethane, ClCHMe$_2$, and ClCH$_2$CO$_2$Me, and iodobenzene, also react with K[Rh(IPr)(dvtms)] (K[**1**]), but these reactions produce mixtures of products. In all cases, the rhodium(0) complex [Rh(IPr)(dvtms)] (**3**) was consistently detected by NMR if using a 1:1 molar ratio (Scheme 1).
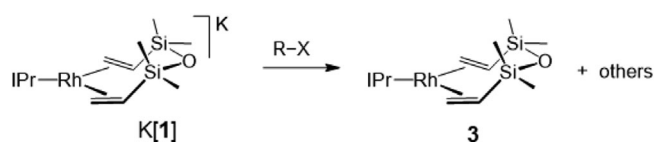
Scheme 1. Reactions of K[**1**] with R–X (CH$_2$Cl$_2$, ClCHMe$_2$, ClCH$_2$CO$_2$Me, IPh).
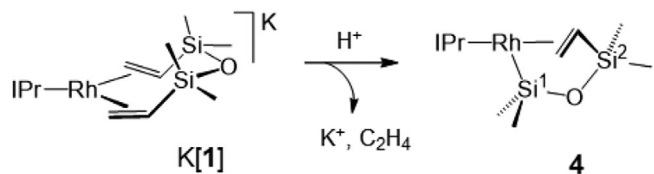
Scheme 2. Reactions of K[**1**] with proton sources giving **4** and ethylene.

This fact suggests that these reactions proceed via one-electron oxidation rather than oxidative addition.

The likely mechanism involves a nucleophilic attack by the metal on the carbon bonded to the halogen, transferring one electron to give potassium halide along with two radicals: the relatively stable paramagnetic complex **3** and the organic fragment, which then collapses in the solvent cage.

The rarity of TP structures in d^8 complexes led Grüzmacher et al. to propose strategies for stabilizing TP forms as ground-state structures. They suggested that combining cations like a proton or a silyl cation (SiH$_3^+$) with planar d^{10}-ML$_3$ fragments, such as the hypothetical species [Rh(C$_2$H$_4$)$_3$]$^-$, could favor the TP structure. Indeed, DFT calculations confirmed that the TP form, with H or SiH$_3$ at the apex, is significantly more stable than the planar form.[48] In this regard, the synthesis of complex **2** supports this hypothesis.

Following this idea, we reacted complex **1** with stable carbocations, such as the perchlorate salts of triphenylcarbonium and tropylium. The sole product observed by NMR was the rhodium(0) complex [Rh(IPr)(dvtms)] (**3**), indicating that no Rh—C bond formation occurred. Instead, one-electron transfer to the cation took place, generating radicals, which is consistent with the oxidative nature of these carbocations.[50]

Noteworthy, K[**1**] reacts not only with strong acids such as HBF$_4$ but even extracts protons from weak acids, such as water and phenols (MesOH, 2,6-^{t}Bu$_2$C$_6$H$_3$OH). In all cases, the solution color changes from orange to red. The reaction time to achieve completion depends on the proton source's strength.[51] HBF$_4$ completes the reaction in 10 minutes, whereas those with phenols take about 2 hours. Surprisingly, the final product is not a hydride complex but the tricoordinate complex [Rh(IPr)(SiMe$_2$OSiMe$_2$CH = CH$_2$)] (**4**, Scheme 2). This transformation involves Rh—Si bond formation and the removal of one vinyl group from dvtms as ethylene, which was detected by ^{1}H NMR spectroscopy.

The molecular structure of complex **4** (Figure 4) reveals a tricoordinate, T-shaped rhodium(I) center bonded to the C1 carbon of the IPr ligand, to one silicon atom (Si^1), and to a vinyl group from the early dvtms ligand.

The C = C bond of the vinyl group is perpendicular to the rhodium coordination plane. The Rh—Si^1 bond distance (2.2362(7)
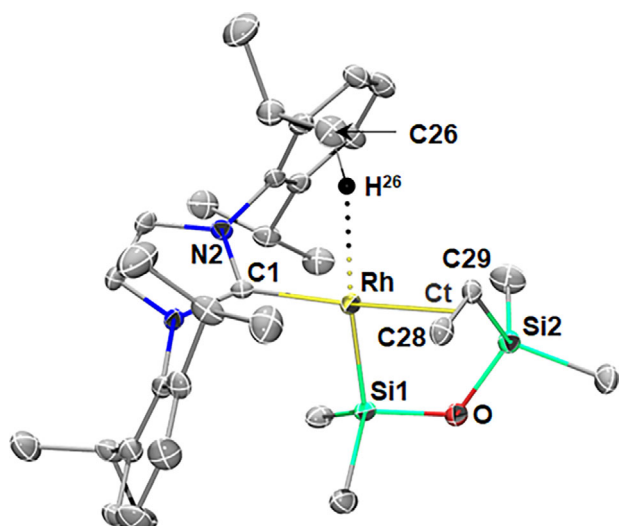
Chemistry–A European Journal

Research Article
doi.org/10.1002/chem.202501877

Chemistry
Europe

European Chemical
Societies Publishing

Figure 4. Molecular structure (ORTEP, ellipsoids set at 50% probability) of complex [Rh(IPr)(SiMe$_2$OSiMe$_2$CH = CH$_2$)] (**4**). Selected bond distances [Å] and angles [°]: Rh − C1 2.041(2), Rh − Ct 2.029(2), Rh − Si1 2.2362(7), C28 − C29 1.399(3), Rh⋯H26 2.449, C1 − Rh − Ct 177.2(1), C1 − Rh − Si1 94.61(7), Si1 − Rh − Ct 91.98(7), Si1 − Rh − H26 173.3.
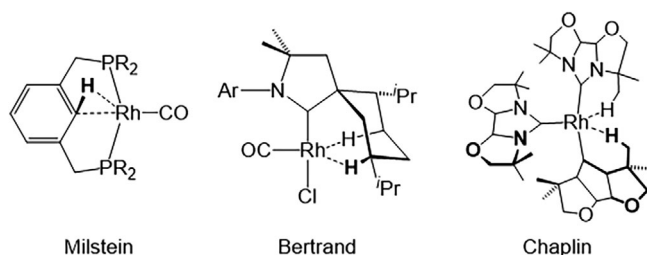

Figure 5. Chemical structures of tricoordinated 14-electron rhodium complexes featuring Rh⋯H interactions.

Å) is notably shorter than those in related rhodium(I) complexes.[52,53] This shorter distance is likely due to the absence of a ligand trans to the Si^1 atom. Alternatively, it could be argued that the strong *trans* influence of silicon prevents the presence of a ligand in this position. In the solid state, a proton from an isopropyl group appears to interact with the rhodium atom at the coordination vacancy. This is supported by the short Rh⋯H26 distance (2.449 Å) and the nearly linear C26—H26⋯Rh angle (152.1°), which align more closely with an anagostic interaction (2.3–2.9 Å, 110–170°) than an agostic one (1.8–2.3 Å, 90–140°), according to the Brookhart definition.[54] However, this interaction could not be detected by ^{1}H NMR, even at − 90 °C in toluene-d$_8$.

Aside from this interaction, complex **4** is an unusual 14-electron species. Related 14-electron complexes reported by Milstein,[55] Bertrand,[56] and Chaplin[57] are shown in Figure 5.

In solution, the "Me$_2$Si^1-Rh" and "Rh-(H$_2$C = CH-Si^{2}Me$_2$)" fragments were clearly identified by their correlation peaks in the ^{1}H,^{29}Si-hmbc spectrum. Si^1 correlated with the methyl protons, whereas Si^2 correlated with the two methyl groups and three olefinic protons. From this 2D spectrum, the ^{29}Si NMR spectrum was obtained, showing a singlet for Si^2 at $\delta = -1.9$ and a doublet for Si^1 at $\delta = 49.1$ (J(Si,Rh) = 66 Hz), as expected.
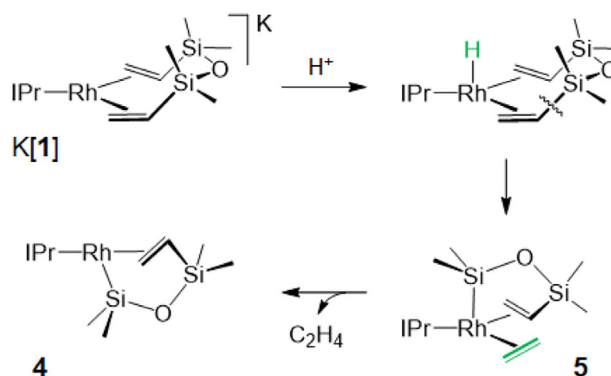
Scheme 3. Proposed elemental steps for the formation of complex **4** from the reaction of K[**1**] with proton sources.

Based on the experimental data and the isolobal analogy between Me$^+$ and H$^+$, the mechanism outlined in Scheme 3 explains the formation of complex **4**. The reaction begins with the protonation of the electron-rich Rh(−I) center, generating the hydride intermediate [Rh(IPr)(dvtms)(H)], which resembles the structure of the methyl complex **2**. In the next step, an anti-Markovnikov addition of the hydride to the vinyl group occurs, leading to the cleavage of the Si—C bond. This results in the release of ethylene and the formation of a new Rh—Si bond.

The intermediate complex **5**, detected by NMR, then undergoes ethylene elimination to form complex **4**. Herein, the hydride clearly migrates to the more electronegative carbon (as shown above), which strongly indicates an electrophilic character (δ^+) of the hydride attached to the rhodium(I) center. However, direct protonation of the olefin to produce directly complex **5** cannot be definitively ruled out.

DFT calculations show that transformation of the hydride complex [Rh(IPr)(dvtms)(H)] into **5** is only slightly endergonic by 2.3 kcal mol^{-1} and that elimination of ethylene on going from **5** to **4** is thermodynamically favored by 3.8 kcal mol^{-1}.

Monitoring the reaction of K[**1**] with water (in a 1:1 molar ratio) at − 60 °C in d$_8$-toluene revealed the presence of the intermediate [Rh(IPr)(SiMe$_2$OSiMe$_2$CH = CH$_2$)(H$_2$C = CH$_2$)] (**5**, Scheme 3) featuring coordinated ethylene in the reaction mixture.

Thus, two sets of olefinic resonances were identified through selective ^{1}H-seltocsy experiments (Figure 6). The red trace corresponds to the vinylic H$_2$C = CH − OSi^2 moiety, whereas that in green corresponds to ethylene. Both C = C bonds are attached to rhodium, as confirmed by the doublet signals of their carbon nuclei due to coupling with ^{103}Rh in the ^{13}C{^{1}H} NMR spectrum.

Additionally, the ^{1}H,^{29}Si-hmbc NMR spectrum displayed two silicon signals with chemical shifts of $\delta = 2.1$ and 48.7 ppm, similar to those observed in complex **4**. The low-field signal corresponds to Si^1, directly bonded to rhodium, as indicated by a large J(Si,Rh) coupling constant of 45 Hz.

Complex K[**1**] also reacts with other electrophiles, including aldehydes and ketones. However, its strong proton affinity prevails, abstracting protons from enolizable compounds such as acetone, butanone, methylisobutylketone, and isobutyraldehyde to give complex **5** and the corresponding enolate (confirmed on monitoring the reactions by ^{1}H NMR in C$_6$D$_6$).
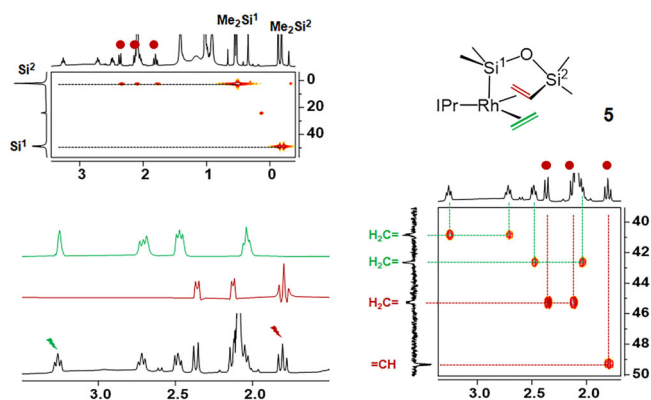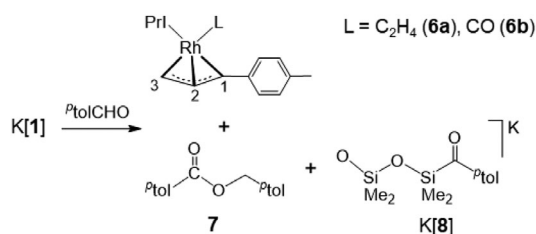
Figure 6. Selected regions of the ^{1}H-seltocsy NMR spectra upon irradiation of the resonances marked with a ray (left, bottom), ^{1}H,^{29}Si-hmbc NMR spectrum (left, top), and ^{1}H,^{13}C-hsqc NMR spectrum (right) of the intermediate **5**.

Figure 7. Molecular structure (ORTEP, ellipsoids set at 50% probability) of complex [Rh(IPr)(η^3-C$_3$H$_4^P$tolyl){(C$_2$H$_4$)/(CO)}] (**6a/6b**). Selected bond distances [Å] and angles [°]: Rh — C1 2.018(3)/2.015(3), Rh — C35 2.209(4)/2.226(4), Rh — C36 2.124(4)/2.130(4), Rh — C37 2.152(4)/2.162(3), Rh — C40 1.870(7)/1.891(8), Rh — Ct 2.043(6)/2.046(5) C38 — C39 1.376(8)/1.378(6), C1 — Rh — Ct 96.6(2)/95.7(2), C1 — Rh — C35 166.19(15)/165.49(14), Ct — Rh — C37 160.6(2)/161.3(2). Ct is the middle point of the C38 — C39 bond. Only CH carbons of the ^{i}Pr groups are shown for clarity.

Scheme 4. Products from the reaction of K[**1**] with ^{P}tolCHO.

However, reactions of K[**1**] with nonenolizable carbonyl compounds, such as p-methylbenzaldehyde (^{P}tolCHO), follow a distinctive path.

The reaction (Scheme 4) consistently gives [Rh(IPr)(η^3-C$_3$H$_4^P$tolyl)(C$_2$H$_4$)] (**6a**) as the sole rhodium(I) complex, the ester ^{P}tolyl—CO$_2$—CH$_2^P$tolyl (**7**) (identified by NMR[58]), and an oxo-disilyl compound resulting from the conversion of dvtms into products, tentatively identified as K[**8**].

Complex **6a** was isolated as an orange-red solid and fully identified by NMR and X-ray methods. The allyl group exhibits four signals in the ^{1}H NMR spectrum and three resonances in the ^{13}C{^{1}H} NMR spectrum, corresponding to carbons C^1, C^2, and C^3, at δ = 101.8, 70.1, and 46.7 ppm, respectively. These signals appear as doublets due to coupling with the active ^{103}Rh nucleus [J(C,Rh) = 6, 5, and 10 Hz, respectively]. Additionally, the freely rotating ethylene ligand was identified by two signals in the ^{1}H NMR spectrum and a single resonance in the ^{13}C{^{1}H} NMR spectrum at δ = 55.2 ppm [J(C,Rh) = 13 Hz].

Figure 7 shows the molecular structure of [Rh(IPr)(η^3-C$_3$H$_4^P$tolyl)/{(C$_2$H$_4$)/(CO)}] (**6a/6b**), which consists of two similar but independent molecules in the asymmetric unit. Each independent molecule exhibits disorder in one ligand, either ethylene (**6a**) or carbon monoxide (**6b**). In the measured crystal, the populations found were 76.6(5)% of **6a** and 23.4(5)% of **6b**. The key feature in both is the presence of the new anionic ligand, [H$_2$C = CH — CH^{P}tolyl]$^-$, which coordinates to rhodium through the three carbons of the allyl group. The rhodium coordination sphere is completed by the IPr ligand bonded
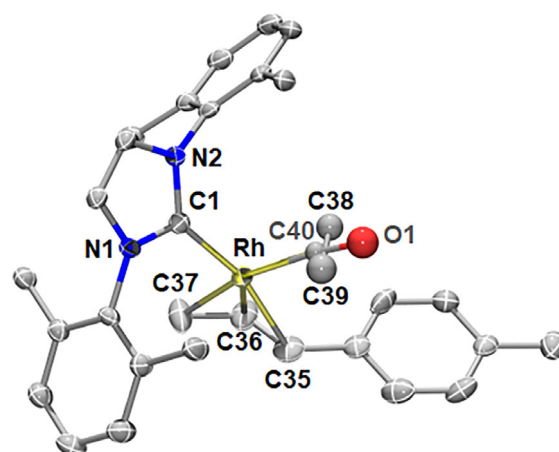
via the C1 carbon, along with either ethylene (in **6a**) or carbon monoxide (in **6b**).

The outcome of the reaction is notably dependent on the K[**1**]:^{P}tolCHO ratio and the way of addition of the aldehyde. In any case, the reaction requires more than two molar-equiv. of aldehyde to reach completion. If aldehyde is added in a slight excess (1:3), a ratio of products **6a**:**7** = 80:20 ensues. Interestingly, if twelve molar-equiv. of aldehyde were added, the ratio was reversed, shifting to **6a**:**7** = 16:84 in 1 hour. This result indicates that the anionic rhodium(−I) complex, K[**1**], behaves as a catalyst, running up to five cycles of the aldehyde condensation before being fully transformed into the inactive complex **6a**.

Further reaction of p-tolylbenzaldehyde with **6a** leads to a slow aldehyde decarbonylation to give [Rh(IPr)(η^3-C$_3$H$_4^P$tolyl)(CO)] (**6b**) and ethylene. The structure of **6b** is similar to **6a**, in which a carbonyl group formally replaces ethylene. In fact, monocrystals grown from the mother liquor of the reaction in the freezer resulted in a mixture of co-crystallized **6a** and **6b**, as disclosed above.

On the other hand, if p-tolybenzaldehyde was added to K[**1**] in a large excess (^{P}tolCHO:K[**1**], 100:1), replacement of dvtms occurs, but neither the ester nor identifiable rhodium products were isolated.

Considering the reaction itself, there are two processes involved: a catalytic cycle and the formation of a rhodium complex, **6a**, inactive as a catalyst. Moreover, these are competitive outcomes, since as the formation of **6a** progresses the catalytic cycle stops. Clearly, both of them possess a common intermediate. Nonetheless, a detailed mechanistic view of the reaction, particularly the pathway to **6a** involving C—C bond formation between a vinyl group and a "^{P}tolCH" fragment (from the aldehyde), represents important challenges. Therefore, we rather
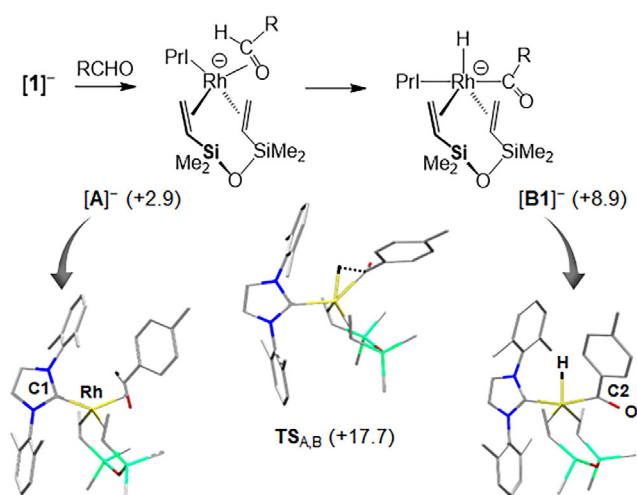
Chemistry–A European Journal

Research Article
doi.org/10.1002/chem.202501877

Chemistry
Europe
European Chemical
Societies Publishing

Figure 8. First steps in the reaction of K[**1**] with *p*-tolylCHO and DFT calculations of intermediates [**A**]$^-$ (left) and [**B1**]$^-$ (right), and **TS**$_{A,B}$ (middle). Values in brackets are given in kcal mol^{-1}. Selected bond distances [Å] and angles [°]. [**A**]$^-$: Rh···H, 2.764; C − H, 1.098; C2 − O, 1.318; **TS**$_{AB}$: Rh···H, 1.720; C − H, 1.362; C2 − O, 1.254; [**B**]$^-$: Rh − H, 1.609; C2 − O, 1.231; C1 − Rh − C2 163.01. R = *p*-tolyl. The methyl groups of ^{i}Pr have been removed for clarity.

Figure 9. Competitive reaction pathways from the common intermediate [**B1**]$^-$, and DFT calculations of intermediates [**C1**]$^-$ (left) and [**D**]$^-$ (right). Values in brackets are given in kcal mol^{-1}.

prefer to offer insights on the mechanism using DFT calculations of selected plausible intermediate species.

Regarding the first step for both reactions, a nucleophilic attack of the metal on the carbonyl group was considered. However, this intermediate is rather described as an adduct of the metal through the C = O bond. Thus, DFT calculations indicate that the interaction of *p*-tolylCHO with K[**1**] gives the η^2-CO coordinated adduct [**A**]$^-$, which is only 2.9 kcal mol^{-1} higher in energy than the separated species ([**1**]$^-$ + *p*-tolylCHO) (Figure 8). In this adduct, rhodium adopts a nearly tetrahedral geometry, consistent with an 18-electron Rh(−I) species. Although rare, such complexes have been observed in related "Ni^0(NHC)" systems.[59]

Notably, the aldehyde proton in [**A**]$^-$ is positioned close to rhodium, thus enabling a C—H bond activation step to give the hydrido-acyl complex [**B1**]$^-$ (Figure 8). Intermediate [**B1**]$^-$ is a rhodium(I) species in a nearly trigonal-bipyramidal environment, with the acyl group and IPr ligand at the *axial* positions and the diolefin and hydride ligands in the *equatorial* positions. This species lies 6.3 kcal mol^{-1} higher in energy than adduct [**A**]$^-$ and is formed through a 14.8 kcal mol^{-1} activation barrier (**TS**$_{A,B}$, Figure 8). This barrier is similar to that reported by Fu and Yu for the aldehyde C − H bond activation on the model complex [Ni^0(NHC)(η^2-aldehyde)$_2$] (14.9 kcal mol^{-1}).[60] The hydride-acyl isomer, in which the hydride and acyl ligands switch positions ([**B2**]$^-$; see Figure S4), is slightly higher in energy than [**B1**]$^-$ by 2.8 kcal/mol^{-1}. Then, species [**B1**]$^-$ is a reasonable proposal for the common intermediate in both reactions.

At this point, it is interesting to mention that whereas the catalytic cycle to the ester requires the diolefin dvtms to remain intact for catalyst regeneration, the pathway to **6a** involves the rupture of both Si—C bonds, yielding two vinyl fragments ("−CH = CH$_2$"); one of them captures a proton to give ethylene, whereas the other binds a "*p*-tolylCH" fragment to form the allyl ligand. Then, starting from the hydride species [**B1**]$^-$, a logical
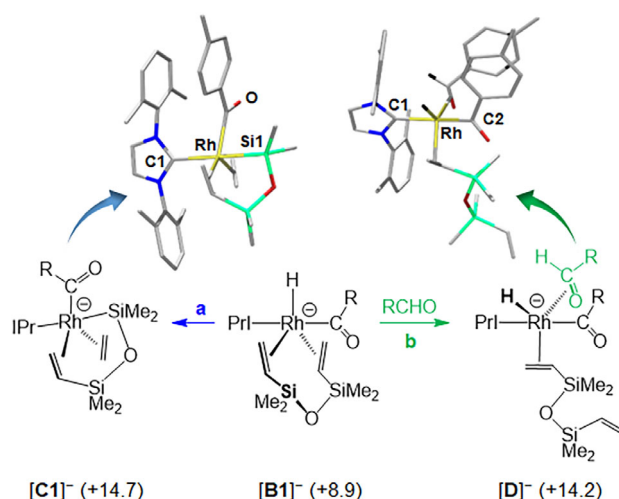
proposal outlining the divergence of these pathways is shown in Figure 9.

Under low aldehyde concentrations, hydride insertion with rupture of the first Si—C bond leads to the formation of [**C1**]$^-$ (path a, in blue). This process (analogous to that described in Scheme 3 for [Rh(H)(IPr)(dvtms)]) generates the ethylene ligand found in [Rh(IPr)(η^3-C$_3$H$_4$^{p}tolyl)(C$_2$H$_4$)] **6a**. Intermediate [**C1**]$^-$ features a trigonal bipyramidal rhodium(I) center in which the C1 carbon of the IPr ligand and Si lie at the apical positions. The silyl-acyl isomer, in which the silyl and acyl ligands switch positions ([**C2**]$^-$ see Figure S4), was found to be higher in energy than [**C1**]$^-$ by 16 kcal/mol^{-1}.

In contrast, under higher aldehyde concentrations, the more likely pathway involves replacement of one of the C = C bonds of dvtms by an additional molecule of aldehyde to give intermediate [**D**]$^-$ (path b, in green). Both intermediates, [**C1**]$^-$ and [**D**]$^-$ were found to have similar energies of 14.7 and 14.2 kcal mol^{-1}, respectively.

The catalytic cycle for aldehyde dimerization (Scheme 5) begins with steps (*i*) and (*ii*), as discussed previously (Figures 8 and 9). Then, intermediate [**D**]$^-$ readily undergoes C = O insertion into the Rh—H bond to give the acyl-alkoxo species [**E1**]$^-$ (step *iii*). The trigonal bipyramidal isomer [**E2**]$^-$ ([Rh(IPr)(η^2-dvtms)(OCH$_2$R)(COR)], see Figure S4) is 7.3 kcal mol^{-1} higher in energy than [**E1**]$^-$, suggesting that the subsequent reductive elimination of OCH$_2$R and COR (step *iv*) is more likely to occur via the square-planar [**E1**]$^-$ isomer. The driving force for this transformation is the re-coordination of the olefin, leading to ester formation and regenerating the Rh(−I) catalyst.

On the whole, this catalytic cycle is quite similar to that DFT-calculated by Fu and Yu for the dimerization of aldehydes with a "Ni^0(NHC)" system.[60]

The way from [**C**]$^-$ to **6a** + K[**8**], which involves the deactivation of the catalyst, is intricate. The best approach we can propose, according to the DFT energies of the implicated species (Scheme 6 and Figure S5), consists of:
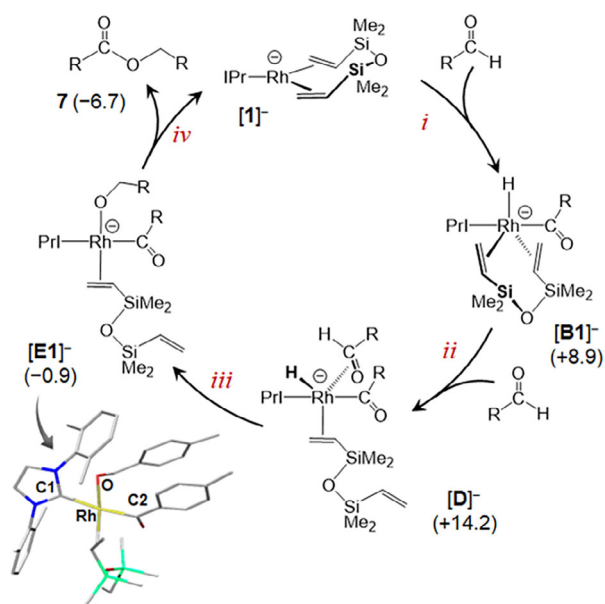
Scheme 5. Plausible catalytic cycle for the Tishchenko reaction catalyzed by complex K[**1**]. R = *p*-tolyl. Values in brackets are given in kcal mol^{-1}.
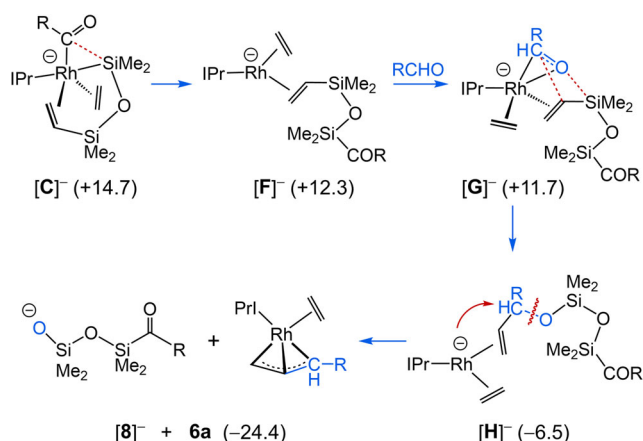
Scheme 6. Proposed steps for the reaction of K[**1**] with *p*-tolCHO from the key intermediate [**B1**]$^-$ to the allyl complex **6a** and K[**8**]. R = *p*-tolyl. Values in brackets are given in kcal mol^{-1}.

(i) reductive elimination of the acyl group via bonding of the oxygen to silicon to give [**F**]$^-$,

(ii) coordination of a new molecule of aldehyde to give [**G**]$^-$,

(iii) concerted attack of the C = O bond with the vinyl − SiMe$_2$ moiety to give [**H**]$^-$, and

(iv) cleavage of the C − O bond associated to the coordination of the allyl group.

Although the transition states could not be calculated, and we admit the proposal is in some way audacious, it has in its favor that the sequence of steps goes in the direction of sliding down the energy.

Finally, the result from the degradation of the dvtms should be the anionic species K[**8**]. DFT calculations support this proposal because it leads to a strong exoenergic change and, certainly, signals from this species can be observed in the ^{1}H NMR spectra of the reaction mixtures. However, we could not

observe the anion in the mass spectra, and therefore it could not be fully identified.

3. Conclusion

In conclusion, we showcase reactions of a rare and coordinatively unsaturated K[Rh^{-1}(IPr)(dvtms)] (K[**1**]) complex. Previous experiments indicated the ability of the metal to bind a Lewis acidic fragment such as [AuPPh$_3$]$^+$. Now, we disclose this behavior as a Brönsted base because of its avidity for protons even from very weak protic acids such as water or enolizable aldehydes or ketones. Moreover, the nucleophilic character of the compound centered on the metal is revealed by the reaction with a typical electrophile such as MeI.

Furthermore, these reactions reveal the feasibility of rhodium(−I) to undergo oxidative additions to form rhodium(I) compounds. Interestingly, the isolated products are a tricoordinated, highly unsaturated complex and a tetracoordinate complex that display an unusual TP structure. Nonetheless, these reactions can be compounded with simple oxidations, as shown by the reactions of (K[**1**]) with alkyl and aryl halides. Finally, reactions of K[**1**] with nonenolizable aldehydes disclosed the ability of rhodium(−I) to behave as a catalyst for the dimerization of aldehydes to esters through a Rh(-I)/Rh(I) catalytic cycle. This reaction becomes more complex because a side reaction of the aldehyde with the divinyltetramethyldisiloxane ligand deactivates the catalyst to give an allylrhodium complex. We propose a common intermediate for both reactions that rationalizes the behavior of the system involving competitive reactions and different products.

Supporting Information

The authors have cited additional references within the Supporting Information.[61–71]

Conflict of Interest

The authors declare no conflict of interest.

Chemistry–A European Journal

Research Article
doi.org/10.1002/chem.202501877

Chemistry Europe
European Chemical
Societies Publishing

Data Availability Statement

The data that support the findings of this study are available from the corresponding author upon reasonable request.

[1] V. R. Landaeta, T. M. Horsley Downie, R. Wolf, *Chem. Rev.* **2024**, *124*, 1323.

[2] A. Noor, *Coord. Chem. Rev.* **2023**, *476*, 214941.

[3] Y. Liu, J. Cheng, L. Deng, *Acc. Chem. Res.* **2020**, *53*, 244.

[4] U. S. D. Paul, U. Radius, *Eur. J. Inorg. Chem.* **2017**, 3362.

[5] S. Roy, K. C. Mondal, H. W. Roesky, *Chem. Res.* **2016**, *49*, 357.

[6] P. P. Power, *Chem. Rev.* **2012**, *112*, 3482.

[7] J. E. Ellis, *Inorg. Chem.* **2006**, *45*, 3167.

[8] J. C. Ott, D. Bürgy, H. Guan, L. H. Gade, *Acc. Chem. Res.* **2022**, *55*, 857.

[9] R. J. Rama, M. T. Martín, R. Peloso, M. C. Nicasio, in *Advances of Organometallic Chemistry*, Vol. 74, (Ed: P. J. Pérez), Academic, Elsevier, **2020**, p. 241.

[10] L. J. Taylor, D. L. Kays, *Dalton Trans.* **2019**, *48*, 12365.

[11] a) [Rh(CO)₄]· by matrix techniques: J. H. B. Chenier, M. Histed, J. A. Howard, H. A. Joly, H. Morris, B. Mile, *Inorg. Chem.* **1989**, *28*, 4114; b) A. B. P. Lever, G. A. Ozin, A. J. L. Hanlan, W. J. Power, H. B. Gray, *Inorg. Chem.* **1979**, *18*, 2088; c) G. A. Ozin, A. J. L. Hanlan, *Inorg. Chem.* **1979**, *18*, 2091.

[12] [Rh(CO)(PPh₃)₃]·: G. Zotti, S. Zecchin, G. Pilloni, *J. Organomet. Chem.* **1983**, *246*, 61.

[13] a) [Rh(dppe)₂]·: K. T. Mueller, A. J. Kunin, S. Greiner, T. Henderson, R. W. Kreilick, R. Eisenberg, *J. Am. Chem. Soc.* **1987**, *109*, 6313; b) A. J. Kunin, E. J. Nanni, R. Eisenberg, *Inorg. Chem.* **1985**, *24*, 1852; c) J. A. Sofranko, R. Eisenberg, J. A. Kampmeier, *J. Am. Chem. Soc.* **1979**, *101*, 1042.

[14] [Rh{P(OⁱPr)₃}₄]·: G. Pilloni, G. Zotti, S. Zecchin, *J. Organomet. Chem.* **1986**, *317*, 357.

[15] a) [Rh(cod)₂]·: J. Orsini, W. E. Geiger, *Organometallics* **1999**, *18*, 1854; b) J. Orsini, W. E. Geiger, *J. Electroanal. Chem.* **1995**, *380*, 83.

[16] B. de Bruin, J. C. Russcher, H. Grützmacher, *J. Organomet. Chem.* **2007**, *692*, 3167.

[17] [Rh(trop₂PPh)(PPh₃)]·: F. F. Puschmann, J. Harmer, D. Stein, H. Rüegger, B. de Bruin, H. Grützmacher, *Angew. Chem. Int. Ed.* **2010**, *49*, 385.

[18] [Rh(L₄)]·: L. Cataldo, S. Choua, T. Berclaz, M. Geoffroy, N. Mézailles, N. Avarvari, F. Mathey, P. Le Floch, *J. Phys. Chem. A* **2002**, *106*, 3017.

[19] a) [Rh(NN)₂]·: H. Căldăraru, M. K. DeArmond, K. W. Hanck, V. E. Sahini, *J. Am. Chem. Soc.* **1976**, *98*, 4455; b) W. A. Fordyce, K. H. Pool, G. A. Crosby, *Inorg. Chem.* **1982**, *21*, 1027.

[20] [Rh{P(OⁱPr)₃}₄]·: G. N. George, S. I. Klein, J. F. Nixon, *Chem. Phys. Lett.* **1984**, *108*, 627.

[21] [Rh(dppf)₂]·: B. Longato, R. Coppo, G. Pilloni, A. Corvaja, A. Toffoletti, G. Bandoli, *J. Organomet. Chem.* **2001**, *637–639*, 710.

[22] a) [Rh(troppᴾʰ)₂]·: S. Deblon, L. Liesum, J. Harmer, H. Schönberg, A. Schweiger, H. Grützmacher, *Chem. Eur. J.* **2002**, *8*, 601; b) H. Schönberg, S. Boulmaâz, M. Wörle, L. Liesum, A. Schweiger, H. Grützmacher, *Angew.Chem. Int. Ed.* **1998**, *37*, 1423.

[23] [Rh{bis(tropp)}]·: C. Laporte, F. Breher, J. Geier, J. Harmer, A. Schweiger, H. Grützmacher, *Angew. Chem. Int. Ed.* **2004**, *43*, 2567.

[24] [Rh(trop₂dad)]·: F. Breher, C. Böhler, G. Frison, J. Harmer, L. Liesum, A. Schweiger, H. Grützmacher, *Chem. Eur. J.* **2003**, *9*, 3859.

[25] [Rh(SiP₃)]⁻: P. J. Nance, N. B. Thompson, P. H. Oyala, J. C. Peters, *Angew. Chem. Int. Ed.* **2019**, *58*, 6220.

[26] [Rh(IPr)(dvtms)]·: V. Varela-Izquierdo, J. A. López, B. de Bruin, C. Tejel, M. A. Ciriano, *Chem. Eur. J.* **2020**, *26*, 3270.

[27] [Rh(triphos)(CO)]⁻: G. G. Johnston, M. C. Baird, *J. Organomet. Chem.* **1986**, *314*, C51.

[28] [Rh(ᴹᵉtroppᴾʰ)₂]⁻: S. Deblon, H. Rüegger, H. Schönberg, S. Loss, V. Gramlich, H. Grützmacher, *New J. Chem.* **2001**, *25*, 83.

[29] [Rh(CO)₄]⁻: P. Chini, S. Martinengo, *Inorg. Chim. Acta* **1969**, *3*, 21.

[30] [Rh(CO)₂(PPh₃)₂]⁻: J. P. Collman, F. D. Vastine, W. R. Roper, *J. Am. Chem. Soc.* **1968**, *90*, 2282.

[31] [Rh(PF₃)₄]⁻: J. F. Nixon, B. Wilkins, D. A. Clement, *J. Chem. Soc. Dalton Trans.* **1974**, 1993.

[32] [Rh(PF₂NMe₂)₄]⁻: D. A. Clement, J. F. Nixon, *J. Chem. Soc., Dalton Trans.* **1973**, 195.

[33] a) [Rh(dppe)₂]⁻: B. Bogdanović, W. Leitner, C. Six, U. Wilczok, K. Wittmann, *Angew. Chem. Int. Ed. Engl.* **1997**, *36*, 502; b) ref. 13b.

[34] [Rh(tmbp)]⁻: N. Mézailles, P. Rosa, L. Ricard, F. Mathey, P. Le Floch, *Organometallics* **2000**, *19*, 2941.

[35] [Rh(dppf)₂]⁻: see ref. 21.

[36] [Rh(troppᴾʰ)₂]⁻: see ref. 22b.

[37] [Rh(ᴹᵉtroppᴾʰ)₂]⁻: see ref. 28.

[38] A family of complexes of general formula [Rh(dxpy)₂]⁻ has been recently characterized 'in situ': A.-C. Kick, T. Weyhermüller, M. Hölscher, N. Kaeffer, W. Leitner, *Angew. Chem. Int. Ed.* **2024**, *63*, e202408356.

[39] M. L. Neville, C. Chan, B. R. Barnett, R. E. Hernandez, C. E. Moore, J. S. Figueroa, *Polyhedron* **2023**, *243*, 116565.

[40] F. Breher, H. Ruëgger, M. Mlakar, M. Rudolph, S. Deblon, H. Schönberg, S. Boulmaâz, J. Thomaier, H. Grützmacher, *Chem. Eur. J.* **2004**, *10*, 641.

[41] J. A. Sofranko, R. Eisenberg, J. A. Kampmeier, Activation of carbon-hydrogen bonds by [Rh(diphos)₂]⁰ *J. Am. Chem. Soc.* **1980**, *102*, 1163.

[42] F. F. Puschmann, H. Grützmacher, B. de Bruin, *J. Am. Chem. Soc.* **2010**, *132*, 73.

[43] a) S. Oishi, *J. Mol. Catal.* **1987**, *39*, 225; b) E. Amouyal, in *Homogeneous Photocatalysis*, Vol. 2, (Ed.: M. Chanon), Wiley, New York, **1997**, p. 264.

[44] M. R. Grochowski, J. Morris, W. W. Brennessel, W. D. Jones, *Organometallics* **2011**, *30*, 5604.

[45] P. Wang, J. Cheng, D. Wang, C. Yang, X. Leng, L. Deng, *Organometallics* **2020**, *39*, 2871.

[46] F. Ferretti, D. R. Ramadan, F. Ragaini, *ChemCatChem* **2019**, *11*, 4450 *and references therein*.

[47] J. T. Moore, C. C. Lu, *J. Am. Chem. Soc.* **2020**, *142*, 11641.

[48] D. Ostendorf, C. Landis, H. Grützmacher, *Angew. Chem. Int. Ed.* **2006**, *45*, 5169.

[49] O. P. E. Townrow, S. B. Duckett, A. S. Weller, J. M. Goicoechea, *Chem. Sci.* **2022**, *13*, 7626.

[50] N. G. Connelly, W. E. Geiger, *Chem. Rev.* **1996**, *96*, 877.

[51] A. Kütt, T. Rodima, J. Saame, E. Raamat, V. Mäemets, I. Kaljurand, I. A. Koppel, R. Y. Garlyauskayte, Y. L. Yagupolskii, L. M. Yagupolskii, E. Bernhardt, H. Willner, I. Leito, *J. Org. Chem.* **2011**, *76*, 391.

[52] L. Zámostná, S. Sander, T. Braun, R. Laubenstein, B. Braun, R. Herrmann, P. Kläring, *Dalton Trans.* **2015**, *44*, 9450.

[53] D. L. Thorn, R. L. Harlow, *Inorg. Chem.* **1990**, *29*, 2017.

[54] M. Brookhart, M. L. H. Green, G. Parkin, *Proc. Natl. Acad. Sci. U. S. A.* **2007**, *104*, 6908.

[55] C. M. Frech, L. J. W. Shimon, D. Milstein, *Organometallics* **2009**, *28*, 1900.

[56] V. Lavallo, Y. Canac, A. DeHope, B. Donnadieu, G. Bertrand, *Angew. Chem. Int. Ed.* **2005**, *44*, 7236.

[57] A. B. Chaplin, *Organometallics* **2014**, *33*, 624.

[58] C. Tejel, M. A. Ciriano, V. Passarelli, *Chem. Eur. J.* **2011**, *17*, 91.

[59] Y. Hoshimoto, M. Ohashi, S. Ogoshi, *J. Am. Chem. Soc.* **2011**, *133*, 4668.

[60] a) H. Yu, Y. Fu, *Chem. Eur. J.* **2012**, *18*, 16765.

[61] Deposition numbers 2440977 (for **2**), 2440976 (for **4**), and 2440978 (for **6a/6b**) contain the supplementary crystallographic data for this paper. These data are provided free of charge by the joint Cambridge Crystallographic Data Centre and Fachinformationszentrum Karlsruhe Access Structures service.

[62] G. M. Sheldrick, SADABS, Bruker AXS, Madison, WI (USA), **1997**.

[63] G. M. Sheldrick, *Acta Cryst* **2015**, *A71*, 3.

[64] G. M. Sheldrick, *Acta Cryst* **2015**, *C71*, 3.

[65] L. J. Farrugia, *J. Appl. Crystallogr.* **2012**, *45*, 849.

[66] Gaussian 09 (Revision D.01): M. J. Frisch, G. W. Trucks, H. B. Schlegel, G. E. Scuseria, M. A. Robb, J. R. Cheeseman, G. Scalmani, V. Barone, B. Mennucci, G. A. Petersson, H. Nakatsuji, M. Caricato, X. Li, H. P. Hratchian, A. F. Izmaylov, J. Bloino, G. Zheng, J. L. Sonnenberg, M. Hada, M. Ehara, K. Toyota, R. Fukuda, J. M. Hasegawa, M. Ishida, T. Nakajima, Y. Honda, O. Kitao, H. Nakai, T. Vreven, J. A. Montgomery Jr., J. E. Peralta, F. Ogliaro, M. Bearpark, J. J. Heyd, E. Brothers, K. N. Kudin, V. N. Staroverov, R. Kobayashi, J. Normand, K. Raghavachari, A. Rendell, J. C. Burant, S. S. Iyengar, J. Tomasi, M. Cossi, N. Rega, J. M. Millam, M. Klene, J. E. Knox, J. B. Cross, V. Bakken, C. Adamo, J. Jaramillo, R. Gomperts, R. E. Stratmann, O. Yazyev, A. J. Austin, R. Cammi, C. Pomelli, J. W. Ochterski, R. L. Martin, K. Morokuma, V. G. Zakrzewski, G. A. Voth, P. Salvador,

J. J. Dannenberg, S. Dapprich, A. D. Daniels, Ö. Farkas, J. B. Foresman, J. V. Ortiz, J. Cioslowski, D. J. Fox, Gaussian, Inc., Wallingford CT, **2011**.

[67] C. Lee, W. Yang, R. G. Parr, *Phys. Rev. B* **1988**, *37*, 785.

[68] A. D. Becke, *J. Chem. Phys.* **1993**, *98*, 1372.

[69] A. D. Becke, *J. Chem. Phys.* **1993**, *98*, 5648.

[70] S. Grimme, J. Antony, S. Ehrlich, H. Krieg, *J. Chem. Phys.* **2010**, *132*, 154104.

[71] L. E. Roy, P. J. Hay, R. L. Martin, *J. Chem. Theory Comput.* **2008**, *4*, 1029.

RESEARCH ARTICLE

The low-coordinated Rh(−I) complex displays a nonconventional reactivity, affording a Rh(I) compound in a trigonal-pyramidal geometry, a rare true metalloradical Rh(0) complex, a highly unsaturated 14 eV complex featuring a Rh — Si bond, and catalyzes a dimerization of aldehydes to the ester through a Rh(-I)/Rh(I) catalytic cycle with catalyst deactivation to an allylrhodium complex.
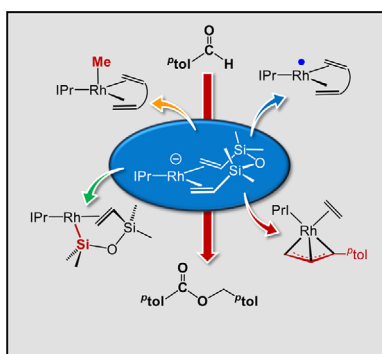
V. Varela-Izquierdo, J. A. López,
M. A. Ciriano, C. Tejel

1 – 9

**A Tour in the Chemistry of a
Tricoordinate Rh(−I) Complex**